JSHC
Japan Society of Histochemistry and Cytochemistry
Established 1959

Acta Histochem. Cytochem. 40 (4): 113–121, 2007
doi:10.1267/ahc.07011

Fragmentation of Protein Kinase N (PKN) in the Hydrocephalic Rat Brain

Norifumi Okii[1], Taku Amano[2], Takahiro Seki[2], Hiroaki Matsubayashi[2], Hideyuki Mukai[3], Yoshitaka Ono[3], Kaoru Kurisu[1] and Norio Sakai[2]

[1]Department of Neurosurgery, Graduate School of Biomedical Sciences, Hiroshima University, [2]Department of Molecular and Pharmacological Neuroscience, Graduate School of Biomedical Sciences, Hiroshima University and [3]Biosignal Research Center, Kobe University

Received April 15, 2007; accepted May 10, 2007; published online July 27, 2007

PKN (protein kinase N; also called protein kinase C-related kinase (PRK-1)), is a serine/threonine protein kinase that is ubiquitously expressed in several organs, including the brain. PKN has a molecular mass of 120 kDa and has two domains, a regulatory and a catalytic domain, in its amino-terminals and carboxyl-terminus, respectively. Although the role of PKN has not been fully elucidated, previous studies have revealed that PKN is cleaved to a constitutively active catalytic fragment of 55 kDa in response to apoptotic signals. Hydrocephalus is a pathological condition caused by insufficient cerebrospinal fluid (CSF) circulation and subsequent excess of CSF in the brain. In this study, in order to elucidate the role of PKN in the pathophysiology of hydrocephalus, we examined PKN fragmentation in hydrocephalic model rats.

Hydrocephalus was induced in rats by injecting kaolin into the cisterna magna. Kaolin-induced rats (n=60) were divided into three groups according to the observation period after treatment (group 1: 3–6 weeks, group 2: 7–12 weeks, and group 3: 13–18 weeks). Sham-treated control rats, injected with sterile saline (n=20), were similarly divided into three groups. Spatial learning ability was estimated by a modified water maze test. Thereafter, brains were cut into slices and ventricular dilatation was estimated. Fragmentation of PKN was observed by Western blotting in samples collected from the parietal cortex, striatum, septal nucleus, hippocampus, and periaqueductal gray matter.

All kaolin-induced rats showed ventricular dilatation. Most of them showed less spatial learning ability than those of sham-treated controls. In most regions, fragmentation of PKN had occurred in a biphasic manner more frequently than that in controls. The appearance of PKN fragmentation in periaqueductal gray matter was correlated with the extent of ventricular dilation and spatial learning disability. These results revealed that PKN fragmentation was observed in rats with kaolin-induced hydrocephalus, models for chronically-damaged brain dysfunction, suggesting that persistent brain insult, such as apoptosis, had occurred in these models. PKN fragmentation could be a hallmark for evaluating morphological and functional damage of the hydrocephalus.

Key words: hydrocephalus, PKN, kaolin, spatial learning, apoptosis

I. Introduction

Hydrocephalus is a pathological condition caused by insufficiency of cerebrospinal fluid (CSF) circulation and subsequent excess of CSF in the brain. The main symptoms of hydrocephalus include motor dysfunction, dementia and urinary incontinence [16]; however, the mechanism by which an excess of CSF causes these symptoms or how these symptoms are compensated remains unclear.

PKN (protein kinase N), also called protein kinase C-related kinase (PRK-1) [26], is a serine/threonine kinase

Correspondence to: Norio Sakai, M.D., Ph.D., Department of Molecular and Pharmacological Neuroscience, Graduate School of Biomedical Sciences, Hiroshima University, Minami-ku, 1–2–3 Kasumi, Hiroshima 734–8551, Japan.
E-mail: nsakai@hiroshima-u.ac.jp

with a molecular mass of 120 kDa that is abundantly expressed in several organs, including the brain. In the brain, the expression of PKN has been confirmed in the cerebellum, hippocampus, limbic cortex, hypothalamus, ventral tegmental area, substantia nigra, pars compacta, raphe neurons, nucleus diagonal band, nucleus basalis, and lateral dorsal tegmental nucleus [7].

PKN possesses a binding site for the small GTP-binding protein Rho in its amino-terminal region and belongs to the family of Rho-activated kinases [1, 15, 29]. Rho participates in various cytoskeleton-dependent cell functions and various cell adhesion events, such as cell migration, cell to cell adhesion, cell morphology (cell rounding) and endoexocytosis of vesicles [11]. Various cytoskeletal proteins have been shown to be substrates of PKN *in vitro*, such as glial fibrillary acidic protein (GFAP) and vimentin [17, 21].

PKN consists of catalytic and regulatory domains, which are located in the carboxyl-terminal and amino-terminal regions, respectively. It is well known that a variety of cellular stresses induce cleavage of PKN at a site between the catalytic and regulatory domains. This process allows the catalytic carboxyl-terminal region of PKN with a size of 55 kDa to be constitutively active. Based on the finding that cleavage of PKN is accelerated when the apoptotic signaling pathway is activated [5, 26], it has been clarified that PKN is proteolytically cleaved by caspase-3, the final executor of apoptosis [5], or related proteases by apoptotic stimulus. A constitutively active fragment has been found to be generated not only in cultured cells [26] but also in an ischemia/reperfusion model of the rat retina [25] and brain [28]. It has also been reported that PKN was accumulated in Alzheimer neurofibrillary tangles [12]. Although accumulating evidence suggests that PKN is involved in the pathogenesis of various neurological disorders, the physiological role of PKN in the central nervous system has not been fully elucidated; especially, its role in hydrocephalus, chronic brain insult, remains unclear.

In the present study, to clarify how the pathological state of hydrocephalus progresses or is compensated, we investigated the role of PKN in this disorder, focusing on the role of cleaved PKN in the pathophysiology of hydrocephalus.

II. Materials and Methods

Induction of hydrocephalus

We produced kaolin-induced hydrocephalus rats according to methods described previously [27]. In brief, 60 adult Wistar rats (body weight of 250–300 g, purchased from Seac Yoshitomi Ltd., Japan) were intraperitoneally anesthetized with pentobarbital (40 mg/kg body weight), and 0.03 ml–0.05 ml of 5% kaolin solution (Sigma Chemical Co., St. Louis, MO) was manually injected into the cisterna magna with the aid of an operating microscope [27].

The animals were divided into three experimental groups according to the period after kaolin injection: 3–6 weeks after kaolin injection (group 1, n=15), 7–12 weeks (group 2, n=30) and 13–18 weeks (group 3, n=15). The same volume of sterile saline was injected in a similar manner into control animals (n=20). These sham-treated control animals were divided into the same manner as that of grouping for kaolin-induced rats (group 1: n=6, group 2: n=8, group 3: n=6).

Estimation of hydrocephalus

Rats with kaolin-induced hydrocephalus were deeply and intraperitoneally anesthetized with pentobarbital (over 40 mg/kg) and then decapitated. Removed brain tissues were cut into 2-mm-thick slices in coronal sections with a brain slicer (RBS-2.0, Aster Industries Inc., Pittsburgh, PA, USA, obtained from Neuroscience Inc., Tokyo, Japan). The magnitude of ventricular dilatation was estimated in coronal slices at the level where the anterior commissure clearly appeared.

The magnitudes of ventricular dilatation were estimated by the ratio of lateral ventricle width (V) to full-length of coronal slice (C) as shown in Figure 1A. V is the width of the lateral ventricle at the levels of the Monro foramen (Fig. 1A). Average values of C and V, obtained from sequential coronal sections in which the anterior commissure was clearly identified, were used for calculating V/C.

Representative brain slices of control and hydrocephalic rat were stained by a Kluver-Barrera method and are shown in Figure 1B.

All experiments were carried out according to the guidelines of the Animal Welfare Committee of Hiroshima University.

Estimation of spatial learning ability

Spatial learning ability of rats was estimated by a modified water maze test [13]. The maze was a circular, black polyethylene swimming pool of 90 cm in diameter filled with 20±1°C water to a depth of 30 cm. A transparent acryl platform of 8 cm in diameter was submerged 1.0 cm under the water surface level. It was randomly located in the center of four equally-divided quadrant circles (target quadrant).

The test was performed as follows. In the first trial, a flag was placed on the platform as a cue for spatial orientation. Each rat was placed in the pool in a quadrant circle that was not adjacent to the target one. The rats swam freely in the pool and usually found the platform within 60 sec. If the rat could not find the platform, it was picked up and laid on the platform for 120 sec in order to let it memorize the spatial relationship between the platform and the pool. In the second, third and fourth trial, the flag was removed from the platform and rats were tested in a similar manner to the first trial. In the fifth trail, the platform was removed and the rat swam freely for 60 sec. Each trial was performed with five minute intervals. Spatial learning ability was estimated by two parameters. One was whether the rats could find the target platform in the second, third and fourth trials. In this case, the results of water maze tests were classified into two categories, "*good*" if the rat could find the platform without flags and "*poor*" if the rat could not find the platform within

three sequential trials. The other was the time spent in the quadrant circles where the platform was placed, which was estimated in the fifth trial and was represented as the ratio to the total examination periods.

Immunoblotting

The methods used for immunoblotting are described in our previous manuscripts [20, 23, 24]. Tissues of the parietal cortex, striatum, hippocampus, periaqueductal gray matter, and septal nucleus were collected from brain slices under a stereoscopic microscope. Approximately 40 mg of each sample was lysed with 400 µl ice-cold RIPA buffer (10 mM Tris/HCl, pH 7.4, containing 1% Nonidet-40, 0.1% sodium deoxycholate, 0.1% SDS, 150 mM NaCl, 1 mM EDTA, 1 mM PMSF, 20 µg/mL leupepcine) and was sonicated (UR-20P, Tomy Seiko, Tokyo, Japan; output, 4; duty, 50%) 15 times at 4°C. The samples were centrifuged at 15,000×g for 15 min at 4°C, and the supernatant was used for immunoblotting. Sixty µg protein of samples was subjected to 7.5% SDS-PAGE, and the separated proteins were electrophoretically transferred onto a polyvinylidine difluoride (PVDF) filter (Millipore, Bedford, MA, USA) [14]. Non-specific binding to the PVDF filter was blocked by incubation with 5% skim milk and 5% normal goat serum in 0.01 M phosphate-buffered saline containing 0.03% Triton-X 100 (PBS-T) for one hour. The filters were then incubated with a primary antibody against PKN C-terminus (C6, diluted 1:4000), provided by Dr. H. Mukai [22], for one hour at room temperature (RT). After washing with PBS-T, the filters were incubated with peroxidase-conjugated secondary antibody against rabbit IgG (Jackson Immuno-Research Laboratories, West Grove, PA, USA) for an additional one hour. After three rinses, the immunoreactive bands were visualized with a chemiluminescence detection kit (ECL™ Western Blotting Detection Reagents, Amersham Biosciences, Buckinghamshire, England) according to the manufacturer's standard procedure. The rAF3 protein, a recombinant PKN catalytic domain, corresponding to amino acid numbers 561–942 of PKN [28], was expressed in COS7 cells, and was used as an internal control to confirm the cleaved PKN fragment of 55 kDa. The same amount of protein samples containing rAF3 protein was applied in all experiments. The density of the immunoreactive bands of 55 kDa was semi-quantitatively measured by NIH image soft-

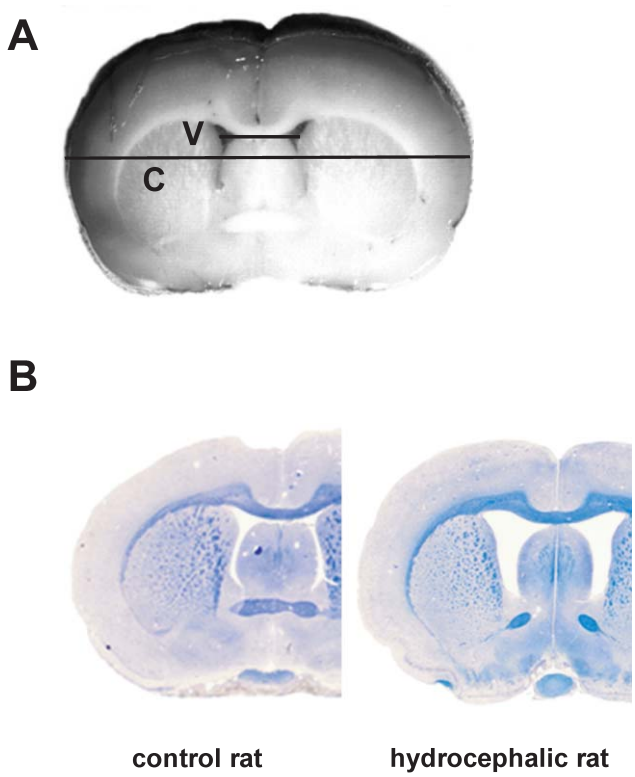

Fig. 1. **A.** Methods for estimation of ventricle dilatation. The brain was cut into 2-mm-thick slices in coronal sections with a brain slicer as described in Materials and Methods. The magnitude of ventricular dilatation was estimated in coronal slices at the level where the anterior commissure clearly appeared. In sequential sections in which the anterior commissure was clearly observed, averaged width of the lateral ventricle, indicated as V, and averaged full-length of coronal slices, indicated as C, were measured. The magnitude of ventricular dilatation was represented as V/C. **B.** Representative coronal sections of hydrocephalic rat and control rat (Kluver-Barrera stain).

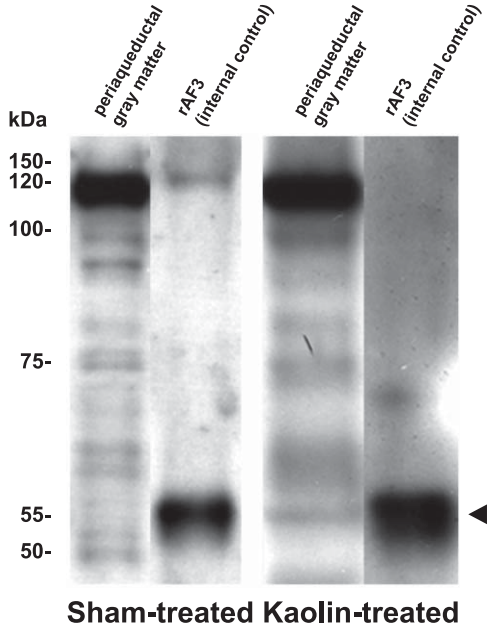

Fig. 2. Representative results of immunoblotting revealing the cleaved 55-kDa PKN fragment. Western blotting results of a sham-treated rat brain (Lt) and a kaolin-induced rat brain (Rt) are shown. Samples for immunoblotting were obtained 4 weeks after the kaolin or sham treatment in this experiment. In sham-treated rats, no or faint fragments of 55-kDa PKN were seen, while the fragments were clearly observed in kaolin-induced rats as indicated by the arrowhead. The molecular size of the fragment corresponds to that of the internal control, recombinant PKN catalytic region that was expressed in COS-7 cells (rAF3).

ware. When the density of the 55-kDa band was 0.05-times larger than that of the internal control, the cleaved PKN fragment was considered to exist (yes).

Representative results of immunoblotting revealing the cleaved PKN fragment of 55 kDa are shown in Figure 2.

III. Results

Treatment with kaolin induced dilatation of the ventricle (Fig. 3)

First, we examined whether treatment with kaolin induced prominent hydrocephalus in our experimental conditions. As shown in Figure 3, kaolin treatment induced significant dilatation of the ventricle in all periods after injection of the drug compared with that in the control sham-treated group. Based on these findings, we used these kaolin-induced rats as reliable hydrocephalus models in later studies.

Kaolin treatment resulted in generation of PKN fragments with a molecular mass of 55 kDa (Table 1)

We examined dissected samples of the parietal cortex, striatum, hippocampus, septal nucleus and periaqueductal gray matter prepared from kaolin-induced and sham-treated rats. As shown in Table 1, in sham-treated control rats, PKN fragments of 55 kDa were rarely observed in most of the regions and periods examined except in the hippocampus. In the hippocampus, 30–40% of the samples contained fragmented PKN in all periods. In contrast, in kaolin-induced rats, 55-kDa PKN fragments were more frequently seen in the parietal cortex, hippocampus, septal nucleus and periaqueductal gray matter, compared with matched control sham-treated rats. (Statistical significance is indicated as "*a*" in Table 1.)

The rate of appearance of PKN fragments seemed to be less in the period of 7–12 weeks after kaolin injection than in the periods of 3–6 weeks and 13–18 weeks. In the parietal cortex, striatum and, the rate of appearance in the period of 7–12 weeks was significantly less than that in the period of 3–6 weeks after kaolin injection. (Statistical significance is indicated as "*b*" in Table 1.) The same tendency was observed in other regions, although statistical significance was not obtained. These results indicate that appearance of PKN fragments was biphasic.

Spatial learning ability was impaired in kaolin-induced rats (Fig. 4)

Spatial learning ability was accessed by simplified methods using a water maze as described in Materials and Methods. As shown in Figure 4, the time spent in the quadrant circles where the platform was placed, was significantly decreased in kaolin-induced rats of groups 2 and 3, compared with those in age-matched controls. This finding suggests that spatial learning ability was worsened in kaolin-induced rats. Also, spatial learning ability of rats in group 3 was significantly lower than those in group 2.

To exclude the possibility that the performance in the water maze test was influenced by motor function of rats, we compared the swimming speeds of kaolin-induced and sham-treated rats. The swimming speeds of sham-treated control rats, kaolin-induced rats in group 2 and 3 were 23.1±5.2 (n=18), 23.4±3.5 (n=15) and 24.0±4.2 (n=15) cm/sec (mean±S.E.M), respectively, with no significant

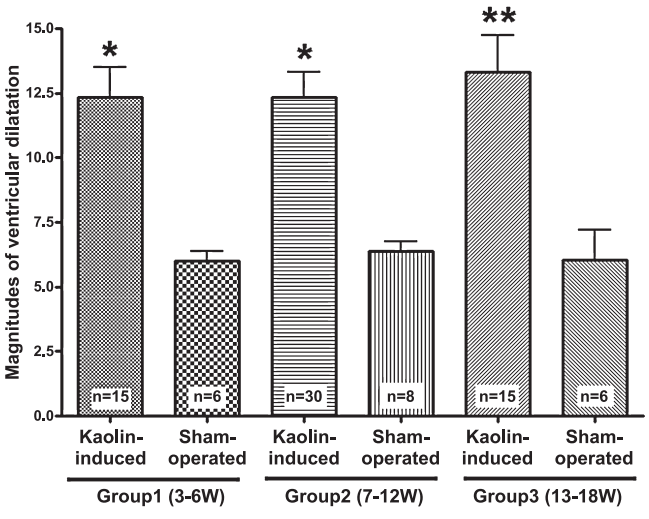

Fig. 3. Ventricular dilatation induced by injection of kaolin. In all groups, the magnitudes of ventricular dilatation of kaolin-treated rats were significantly larger than those of sham-treated rats. (*p<0.01, compared to sham-treated rats, **p<0.05, compared to sham-operated rats, unpaired t-test). Data represent means±SEM.

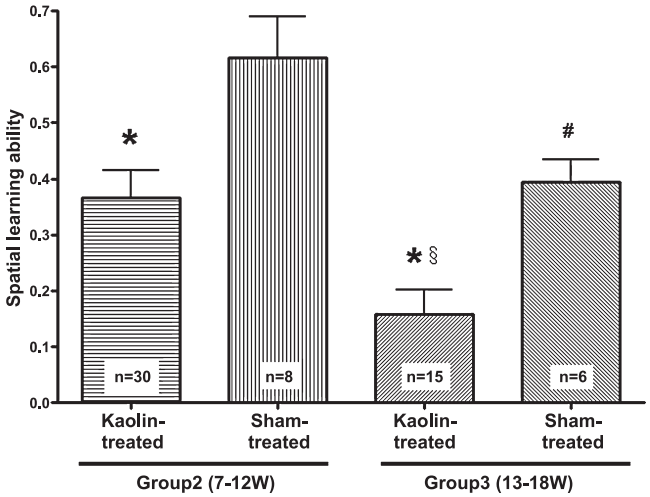

Fig. 4. Spatial learning ability of kaolin-induced and sham-treated rats. Spatial learning ability was evaluated by the time spent in the quadrant circles where the platform was placed as described in Materials and Methods. Spatial learning ability was significantly decreased in kaolin-induced rats (*p<0.01, compared to sham-treated rats, unpaired t-test). Also, the ability of rats in group 3 was significantly lower than that in group 2, both in the case of kaolin-induced and sham-treated rats ($^{\#,\S}$p<0.05, compared to group 2 sham-treated or kaolin-treated rats, respectively, unpaired t-test). Data represent means±SEM.

Table 1. *Presence or absence of 55-kDa PKN fragments in different regions of brain in kaolin-induced and sham-treated rats*

Group	Group 1 (3–6 W)		Group 2 (7–12 W)		Group 3 (13–18 W)	
	Kaolin-induced	Sham-treated	Kaolin-induced	Sham-treated	Kaolin-induced	Sham-treated
Parietal cortex						
55-kDa PKN fragments						
No	5	6	20	7	9	5
Yes	7	0	1	0	1	0
Yes/total (%)	58	0	5	0	10	0
Statistical significance	*		**		**	
Striatum						
55-kDa PKN fragments						
No	4	5	15	6	5	5
Yes	9	1	5	0	5	0
Yes/total (%)	69	20	25	0	50	0
Statistical significance	*		**			
Hippocampus						
55-kDa PKN fragments						
No	0	4	5	4	0	3
Yes	13	2	16	3	10	2
Yes/total (%)	100	33	76	43	100	40
Statistical significance	*				*	
Septal nucleus						
55-kDa PKN fragments						
No	2	5	8	4	2	4
Yes	6	0	11	2	8	1
Yes/total (%)	75	0	58	33	80	20
Statistical significance	*				*	
Periaqueductal gray matter						
55-kDa PKN fragments						
No	3	5	11	6	3	4
Yes	7	0	9	1	7	1
Yes/total (%)	70	0	45	14	70	20
Statistical significance	*					

Samples were prepared from the parietal cortex, striatum, hippocampus, septal nucleus and periaqueductal gray matter of kaolin-induced and sham-treated rats. The appearance of PKN fragments with a molecular mass of 55 kDa was estimated by Western blotting using an anti-PKN antibody against its C-terminus as described in Materials and Methods. "No" or "Yes" represents the presence or absence of 55-kDa PKN fragments in the samples, respectively. The appearance of PKN fragments were compared between kaolin-induced and sham-treated rats in each group and also among groups. Statistical significance was estimated using Fisher's exact probability test. P value less than 0.05 was considered to be statistically significant. In each group, significant difference ($p<0.05$) between kaolin-induced and age-matched sham-treated rats is indicated as "*" in the table. Significant difference ($p<0.05$), compared with kaolin-induced rats in group 1 is indicated as "**". "Yes/total (%)" the rate of appearance of 55-kDa PKN fragments in each group.

In sham-treated rats, PKN fragmentation was rarely seen in most regions except the hippocampus. In kaolin-induced rats, samples of the parietal cortex, hippocampus, septal nucleus and periaqueductal gray matter contained 55-kDa PKN fragments more frequently than did samples of these brain regions from age-matched sham-treated control rats (*). In kaolin-induced rats of group 2, 55-kDa PKN significantly appeared less frequently in parietal cortex and striatum samples than in samples of the same brain regions from rats in group 1 (**).

difference between values for control and kaolin-induced rats, indicating that swimming ability did not differ. In this study, rats in group 1 were not subjected to the water maze test in order to exclude the possibility that surgical damage affects the results of the test.

Appearance of PKN fragments in periaqueductal gray matter of kaolin-induced rats was correlated with the extent of ventricular dilatation (Fig. 5)

The correlation between ventricular dilatation and appearance of 55-kDa PKN fragments was examined using data obtained from kaolin-induced rats in groups 1, 2 and 3. As shown in Figure 5, rats which had PKN fragmentation in the periaqueductal gray matter revealed significantly larger magnitude of ventricular dilation than rats which had no

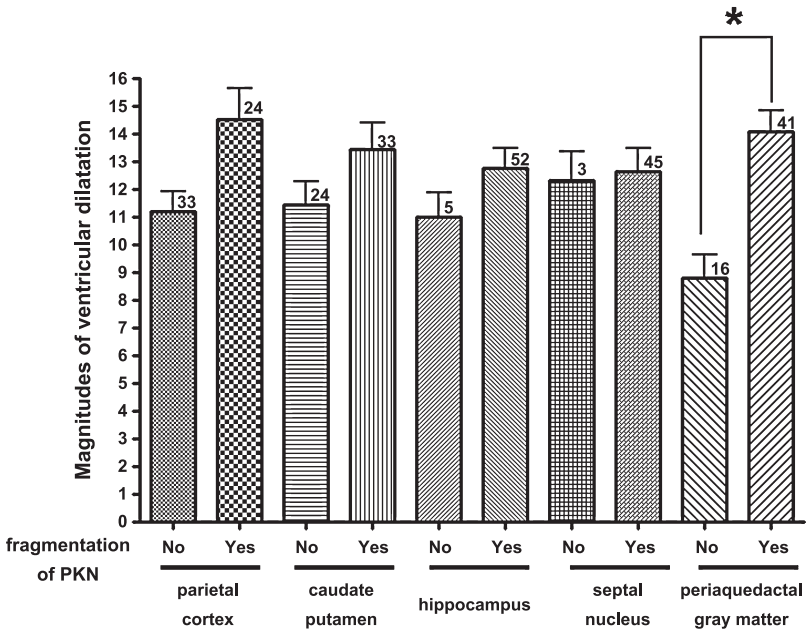

Fig. 5. Correlation between ventricular dilatation and PKN fragmentation in kaolin-induced rats. The correlation between the appearance of PKN fragmentation and the magnitude of ventricular dilation is shown. The magnitude of ventricular dilation was significantly greater in rats that had PKN fragmentation in periaqueductal gray matter, compared to those that had no fragmentation in the area (*p<0.01, unpaired t-test). Digits represent the number of examinations. Data represent means±SEM.

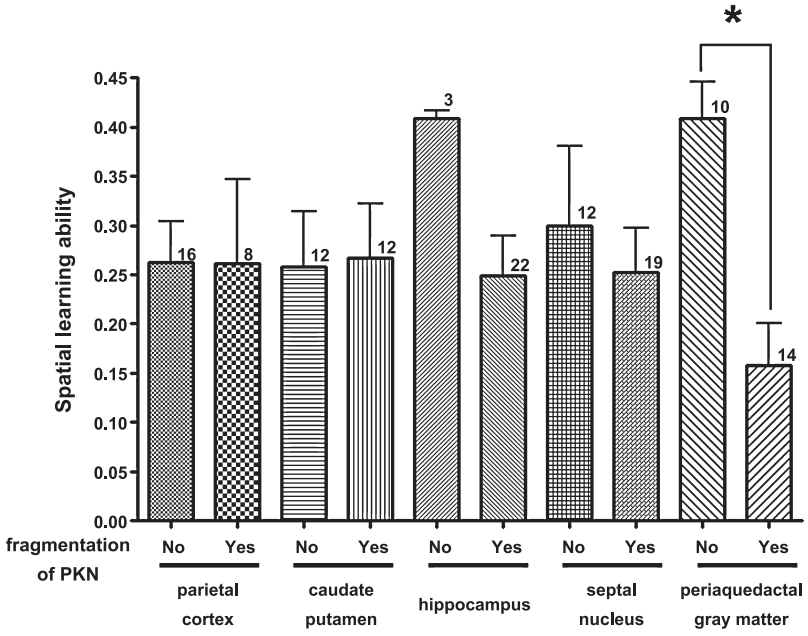

Fig. 6. Correlation between special learning and PKN fragmentation in kaolin-induced rats. Spatial learning ability was evaluated by the time spent in the quadrant circles where the platform was placed, as described in Materials and Methods. The ability was significantly worsened in rats with PKN fragmentations of periaqueductal gray matter, compared to those without them (*p<0.01, unpaired t-test). Digits represent the number of examinations. Data represent means±SEM.

fragmentation (p<0.05, unpaired t-test). In regions other than the periaqueductal gray matter, there was no significant correlation between ventricular dilatation and appearance of PKN fragments. These results suggest that PKN fragmentation occurred in accordance with ventricular dilatation, at least in the periaqueductal gray matter.

Appearance of PKN fragments in periaqueductal gray matter of kaolin-induced rats was correlated with spatial learning ability (Table 2) (Fig. 6)

The correlation between results of the water maze test and appearance of 55-kDa PKN fragments was also examined using data obtained from kaolin-induced rats in group 2 and 3. As shown in Table 2, in the periaqueductal gray matter, 55-kDa PKN fragments were more frequently observed in kaolin-induced rats with "*poor*" results of the water maze test than in those with "*good*" results (indicated as (*a*), $p<0.05$, Fisher's exact probability test). In addition, spatial learning ability, which was estimated by the time spent in the target quadrant circles in the fifth trial as described in Materials and Methods, was significantly lower in rats with 55-kDa PKN fragments of periaqueductal gray matter than those without them (Fig. 6). There was no significant correlation between spatial learning ability and appearance of PKN fragments in brain regions other than periaqueductal gray matter. These results suggest that PKN fragmentation in the periventricular region could be a hallmark of impaired spatial learning ability in kaolin-induced rats.

Table 2. *Relationship between results of water maze test and PKN fragmentation in kaolin-induced rats*

Parietal cortex	Water maze test	
	poor	good
Parietal cortex		
55-kDa PKN fragments		
No	5	12
Yes	1	1
Striatum		
55-kDa PKN fragments		
No	4	9
Yes	2	4
Hippocampus		
55-kDa PKN fragments		
No	0	3
Yes	6	10
Septal nucleus		
55-kDa PKN fragments		
No	1	3
Yes	5	8
Periaqueductal gray matter *		
55-kD PKN fragments		
No	1	10
Yes	5	3

The correlation between results of the water maze test and appearance of 55-kDa PKN fragments was examined. The appearance of 55-kDa PKN fragments in each brain region is redistributed in accordance with results of the water maze test defined in Materials and Methods. A comparison was made between groups with poor and good results. The statistical significance was estimated using Fisher's exact probability test. In periaqueductal gray matter, 55-kDa PKN fragments appeared more frequently in kaolin-induced rats with poor results than in those with good results ($p<0.05$, indicated as "*"). In other brain regions, no statistically significant difference was observed.

IV. Discussion

Adequacy of kaolin-induced rat used in our study as a model for hydrocephalus

In this study, kaolin-induced rats survived with persistent ventricular dilatation up to 18 weeks. To our knowledge, there are only a few reports that observe the extent of ventricular dilatation for an extended period of time after kaolin treatment [2, 10]. However, the ventricular dilatation seemed to progress mildly in our kaolin-induced rats compared with that in previously reported kaolin-induced models [3]. This difference may be due to the amount of injected kaolin used in our experiments because the progression of hydrocephalus is affected by inflammatory damage of the subarachnoid space, which is defined by the amount of injected kaolin. In the prototype kaolin-induced hydrocephalic rats [3], 0.05 to 0.1 ml of 5% kaolin was used while we used 0.03 to 0.05 ml of 5% kaolin, which probably caused the relatively mild damage to circulation of cerebrospinal fluid. In addition, it has been pointed out that ventricular dilatation was affected by the age of rats used. Ding *et al.* reported that more prominent hydrocephalus was induced by kaolin in 6-week-old rats than in 10-week-old rats [3]. In our experiments, we used 10-week-old rats, which would be another reason why our model showed mild ventricular dilatation.

In spite of the mildness of ventricular dilatation, our rats showed apparent impairment in spatial learning ability in addition to morphological change in brain architecture. These findings are comparable with symptoms commonly seen in patients with acquired hydrocephalus, suggesting that the kaolin-induced rats used in our study are adequate models for hydrocephalus. Furthermore, our model is suitable for long-term observation of PKN fragmentation in response to chronic brain damage because mild ventricular dilatation allows rats to survive for an extended period of time.

PKN fragmentation

In the present study, appearance of PKN fragments persisted for up to 18 weeks (126 days) after injection of kaolin. In a previous study, Ueyama *et al.* observed PKN fragmentation up to 28 days after experimental ischemic insult [28]. Chronic damage caused by hydrocephalus may induce persistent PKN fragmentation. It is notable that PKN fragmentation occurs not only via acute brain damage such as ischemia but also via chronic damage such as hydrocephalus as shown in this study. In addition, our results led to the possibility that chronic brain damage caused by hydrocephalus induces persistent apoptosis because PKN fragmentation is a possible hallmark of apoptosis [5, 25, 26].

As shown in Table 1, PKN fragmentation appeared in a biphasic pattern in kaolin-induced rats although it was observed throughout the period examined; that is, the transient-

ly elevated rate of PKN fragment appearance decreased during a period from 6 to 12 weeks after kaolin injection and then increased again during the period from 13 to 18 weeks after the treatment. Since ventricular dilatation did not show such a pattern, this biphasic pattern seen in the appearance of PKN fragmentation is not due to improvement of hydrocephalus. One possible explanation is that the origins of PKN fragments detected during the early and later periods after kaolin injection are different. According to a report by Sumioka *et al.*, PKN fragments, which were thought to be derived from neuronal cells, started to appear 3–5 days after transient ischemic insult of the retina [25]. In contrast, Ueyama *et al.* reported that PKN fragmentation, which was thought to be derived from microglia, start to be elevated at 5 days but was sustained at high levels up to 28 days after transient middle cerebral artery occlusion [28]. These findings suggest that PKN fragments, which were seen in the later phase in our experiments, may originate from microglia. Another possible explanation is that the brain region affected by kaolin-induced hydrocephalus depends on the period after treatment. In the early period, brain damage is caused by high intracranial pressure. However, after intracranial pressure is compensated, chronic hydrocephalus with normal pressure influences the brain damage in the later period [4, 6, 8, 9, 18, 19]. That would be another possible reason why the PKN fragmentation occurred in a biphasic manner.

Correlation of PKN fragmentation with ventricular dilatation and functional impairment

We investigated the relationship between PKN fragmentation and impairment that were morphologically and functionally observed in this study in order to elucidate which parameters of hydrocephalus are correlated with regional PKN fragmentation. As shown in Figures 5, 6 and Table 2, PKN fragmentation in periaqueductal gray matter was correlated with extent of ventricular dilatation and impaired spatial learning ability. Periaqueductal gray matter may be the region most vulnerable to hydrocephalus because it is very close to the cerebral aqueduct. These results suggest that PKN fragmentation in this area is a hallmark for estimating the extent of ventricular dilatation and impairment of spatial learning ability, although it is unlikely that periaqueductal gray matter is involved in the formation of spatial learning. In addition, as shown in Figure 4, spatial learning ability was significantly decreased by aging. Furthermore, in periaqueductal gray matter of sham-treated control rats, appearance of PKN fragmentation tended to increase in accordance with aging (Table 1). This might be another reason why PKN fragmentation was correlated with spatial learning ability in this area.

Contrary to our expectation, PKN fragmentation in the hippocampus, the function of which is involved in spatial learning, was not correlated with any parameters of hydrocephalus. As shown in Table 1, PKN fragmentation occurred at a relatively high rate even in hippocampus of control sham-treated rats. That would mask its direct correlation with spatial learning ability.

V. Conclusion

PKN fragmentation was observed in rats with kaolin-induced hydrocephalus, a chronically-damaged model of brain dysfunction, suggesting that persistent cellular processes, such as apoptosis, occurred in these models. PKN fragmentation could be a hallmark for evaluating morphological and functional damage caused by hydrocephalus. In the present study, the physiological roles of PKN fragmentation in hydrocephalus were not elucidated. Therefore, at present, it is not clear whether fragmented PKN is a factor that exacerbates or improves the progression of hydrocephalus. Studies using knockout mice would help to resolve these issues.

In conclusion, the present findings provide new insights into the pathophysiological understanding of hydrocephalus.

VI. Acknowledgments

This study was supported in part by a Grant-in-Aid for Scientific Research from the Ministry of Education, Sports and Culture and by grants from Takeda Science Foundation, the Uehara Memorial Foundation, the Naito Foundation, and the Japanese Smoking Research Association. This work was carried out using equipment at the Analysis Center of Life Science and Research Facilities for Laboratory Animal Science, Natural Science Center for Basic Research and Development, Hiroshima University and the Research Center for Molecular Medicine, Hiroshima University School of Medicine.

VII. References

1. Amano, M., Mukai, H., Ono, Y., Chihara, K., Matsui, T., Hamajima, Y., Okawa, K., Iwamatsu, A. and Kaibuchi, K. (1996) Identification of a putative target for Rho as the serine-threonine kinase protein kinase N. *Science* 271; 648–650.
2. Del Bigio, M. R., Wilson, M. J. and Enno, T. (2003) Chronic hydrocephalus in rats and humans: white matter loss and behavior changes. *Ann. Neurol.* 53; 337–346.
3. Ding, Y., McAllister, J. P., 2nd, Yao, B., Yan, N. and Canady, A. I. (2001) Neuron tolerance during hydrocephalus. *Neuroscience* 106; 659–667.
4. Edvinsson, L. and West, K. (1971) Relation between intracranial pressure and ventricular size at various stages of experimental hydrocephalus. *Acta Neurol. Scand.* 47; 451–457.
5. Enari, M., Sakahira, H., Yokoyama, H., Okawa, K., Iwamatsu, A. and Nagata, S. (1998) A caspase-activated DNase that degrades DNA during apoptosis, and its inhibitor ICAD. *Nature* 391; 43–50.
6. Gonzalez-Darder, J., Barbera, J., Cerda-Nicolas, M., Segura, D., Broseta, J. and Barcia-Salorio, J. L. (1984) Sequential morphological and functional changes in kaolin-induced hydrocephalus. *J. Neurosurg.* 61; 918–924.
7. Hashimoto, T., Mukai, H., Kawamata, T., Taniguchi, T., Ono, Y. and Tanaka, C. (1998) Localization of PKN mRNA in the rat brain. *Brain Res. Mol. Brain Res.* 59; 143–153.

8. Hiratsuka, H., Tabata, H., Tsuruoka, S., Aoyagi, M., Okada, K. and Inaba, Y. (1982) Evaluation of periventricular hypodensity in experimental hydrocephalus by metrizamide CT ventriculography. *J. Neurosurg.* 56; 235–240.
9. Hochwald, G. M., Boal, R. D., Marlin, A. E. and Kumar, A. J. (1975) Changes in regional blood-flow and water content of brain and spinal cord in acute and chronic experimental hydrocephalus. *Dev. Med. Child Neurol. Suppl.* 35; 42–50.
10. Irigoin, C., Rodriguez, E. M., Heinrichs, M., Frese, K., Herzog, S., Oksche, A. and Rott, R. (1990) Immunocytochemical study of the subcommissural organ of rats with induced postnatal hydrocephalus. *Exp. Brain Res.* 82; 384–392.
11. Kaibuchi, K., Kuroda, S. and Amano, M. (1999) Regulation of the cytoskeleton and cell adhesion by the Rho family GTPases in mammalian cells. *Annu. Rev. Biochem.* 68; 459–486.
12. Kawamata, T., Taniguchi, T., Mukai, H., Kitagawa, M., Hashimoto, T., Maeda, K., Ono, Y. and Tanaka, C. (1998) A protein kinase, PKN, accumulates in Alzheimer neurofibrillary tangles and associated endoplasmic reticulum-derived vesicles and phosphorylates tau protein. *J. Neurosci.* 18; 7402–7410.
13. Kraemer, P. J., Brown, R. W., Baldwin, S. A. and Scheff, S. W. (1996) Validation of a single-day Morris Water Maze procedure used to assess cognitive deficits associated with brain damage. *Brain Res. Bull.* 39; 17–22.
14. Laemmli, U. K. (1970) Cleavage of structural proteins during the assembly of the head of bacteriophage T4. *Nature* 227; 680–685.
15. Maesaki, R., Ihara, K., Shimizu, T., Kuroda, S., Kaibuchi, K. and Hakoshima, T. (1999) The structural basis of Rho effector recognition revealed by the crystal structure of human RhoA complexed with the effector domain of PKN/PRK1. *Mol. Cell* 4; 793–803.
16. Matsumoto, S. and Tamaki, N. (1992) Hydrocephalus. Neuron Publishing Co., Ltd., Tokyo, pp. 81–90.
17. Matsuzawa, K., Kosako, H., Inagaki, N., Shibata, H., Mukai, H., Ono, Y., Amano, M., Kaibuchi, K., Matsuura, Y., Azuma, I. and Inagaki, M. (1997) Domain-specific phosphorylation of vimentin and glial fibrillary acidic protein by PKN. *Biochem. Biophys. Res. Commun.* 234; 621–625.
18. Milhorat, T. H., Mosher, M. B., Hammock, M. K. and Murphy, C. F. (1970) Evidence for choroid-pleux absorption in hydrocephalus. *N. Engl. J. Med.* 283; 286–289.
19. Miwa, S., Inagaki, C., Fujiwara, M. and Takaori, S. (1982) The activities of noradrenergic and dopaminergic neuron systems in experimental hydrocephalus. *J. Neurosurg.* 57; 67–73.
20. Mochizuki, H., Amano, T., Seki, T., Matsubayashi, H., Mitsuhata, C., Morita, K., Kitayama, S., Dohi, T., Mishima, H. K. and Sakai, N. (2005) Role of C-terminal region in the functional regulation of rat serotonin transporter (SERT). *Neurochem. Int.* 46; 93–105.
21. Mukai, H., Toshimori, M., Shibata, H., Kitagawa, M., Shimakawa, M., Miyahara, M., Sunakawa, H. and Ono, Y. (1996) PKN associates and phosphorylates the head-rod domain of neurofilament protein. *J. Biol. Chem.* 271; 9816–9822.
22. Mukai, H., Toshimori, M., Shibata, H., Takanaga, H., Kitagawa, M., Miyahara, M., Shimakawa, M. and Ono, Y. (1997) Interaction of PKN with alpha-actinin. *J. Biol. Chem.* 272; 4740–4746.
23. Seki, M., Tanaka, T., Sakai, Y., Fukuchi, T., Abe, H., Nawa, H. and Takei, N. (2005) Muller Cells as a source of brain-derived neurotrophic factor in the retina: noradrenaline upregulates brain-derived neurotrophic factor levels in cultured rat Muller cells. *Neurochem. Res.* 30; 1163–1170.
24. Seki, T., Adachi, N., Ono, Y., Mochizuki, H., Hiramoto, K., Amano, T., Matsubayashi, H., Matsumoto, M., Kawakami, H., Saito, N. and Sakai, N. (2005) Mutant protein kinase Cgamma found in spinocerebellar ataxia type 14 is susceptible to aggregation and causes cell death. *J. Biol. Chem.* 280; 29096–20106.
25. Sumioka, K., Shirai, Y., Sakai, N., Hashimoto, T., Tanaka, C., Yamamoto, M., Takahashi, M., Ono, Y. and Saito, N. (2000) Induction of a 55-kDa PKN cleavage product by ischemia/reperfusion model in the rat retina. *Invest. Ophthalmol. Vis. Sci.* 41; 29–35.
26. Takahashi, M., Mukai, H., Toshimori, M., Miyamoto, M. and Ono, Y. (1998) Proteolytic activation of PKN by caspase-3 or related protease during apoptosis. *Proc. Natl. Acad. Sci. U S A* 95; 11566–11571.
27. Tashiro, Y., Chakrabortty, S., Drake, J. M. and Hattori, T. (1997) Progressive loss of glutamic acid decarboxylase, parvalbumin, and calbindin D28K immunoreactive neurons in the cerebral cortex and hippocampus of adult rat with experimental hydrocephalus. *J. Neurosurg.* 86; 263–271.
28. Ueyama, T., Ren, Y., Sakai, N., Takahashi, M., Ono, Y., Kondoh, T., Tamaki, N. and Saito, N. (2001) Generation of a constitutively active fragment of PKN in microglia/macrophages after middle cerebral artery occlusion in rats. *J. Neurochem.* 79; 903–913.
29. Watanabe, G., Saito, Y., Madaule, P., Ishizaki, T., Fujisawa, K., Morii, N., Mukai, H., Ono, Y., Kakizuka, A. and Narumiya, S. (1996) Protein kinase N (PKN) and PKN-related protein rhophilin as targets of small GTPase Rho. *Science* 271; 645–648.